Optics Letters

Direct detection of super-thermal photon-number statistics in second-harmonic generation

Alessia Allevi[1,*] and Maria Bondani[2]

[1]Department of Science and High Technology, University of Insubria and CNISM U.d.R. Como, Via Valleggio 11, I-22100 Como, Italy
[2]Institute for Photonics and Nanotechnologies, CNR and CNISM U.d.R. Como, Via Valleggio 11, I-22100 Como, Italy
*Corresponding author: alessia.allevi@uninsubria.it

Received 24 April 2015; revised 10 June 2015; accepted 11 June 2015; posted 11 June 2015 (Doc. ID 239759); published 25 June 2015

Changes in the statistical properties of light undergoing second-harmonic generation are investigated in the photon-number-resolving domain. We theoretically demonstrate that when a portion of multimode thermal light produced by parametric down-conversion is up-converted, both the second-harmonics and the residual beam at the fundamental wavelength are endowed with super-thermal photon-number distributions. The experimental results, which were obtained by exploiting the photo-number-resolving capability of hybrid photodetectors, are in excellent agreement with the theoretical expectations.

OCIS codes: (190.4410) Nonlinear optics, parametric processes; (270.5290) Photon statistics; (040.5160) Photodetectors.

http://dx.doi.org/10.1364/OL.40.003089

Second-harmonic generation (SHG) is a well-known nonlinear process that, since its first observation in 1961 [1], has attracted a lot of attention because of its potential applications. Indeed, based on this process, laser light sources at different wavelengths can be realized thus making the investigation of important properties of matter feasible. SHG also represents a technique commonly exploited in the cases in which the light used in the experiments does not match the operating spectral region of the employed detectors [2]. For instance, this happens in imaging systems with infrared light, whose second-harmonics is in the visible region, where silicon-based detectors have their maximum quantum efficiency [3,4]. In classical optics, SHG is also used as an ultrafast correlator, whereas in quantum optics experiments, it has been employed to investigate the temporal correlation properties of twin-beam states [5,6]. However, in general, not all the properties of the fundamental light are preserved in the SHG process: for instance, the photon-number distribution remains invariant if the input light is coherent, but it could change in the case of different incoming distributions [7–9]. This different behavior has been observed in the past for singlemode lasers operating below threshold by using a photomultiplier in the single-photon-counting regime [10].

In this Letter, we demonstrate that if the light generated by parametric down-conversion (PDC) is frequency doubled, the second harmonics is endowed with higher intensity fluctuations leading to super-thermal statistics, and the same property also holds for the residual light at fundamental frequency. We discuss the factors that could limit the observation of such a behavior, especially the number of modes in the fundamental beam and the efficiency of the SHG process. The experimental investigation has been performed by means of a pair of photon-number-resolving detectors able to reliably reconstruct photon-number distributions [11] as well as shot-by-shot photon-number correlations [12].

From the theoretical point of view, given two variables x and $y = f(x)$, in which f is a generic invertible function, the link between the corresponding probability distributions $P(x)$ and $P'(y)$ can be expressed as $P'(y)dy = P(x)dx$ thus giving $P'(y) = P(f^{-1}(y))/[\frac{d}{dx}f(x)]_{x=f^{-1}(y)}$. In the case of SHG, the relation between the intensity of the incoming light, I, and the intensity of the SH light, I_{SH}, is $I_{\mathrm{SH}} = kI^2$, where k represents the conversion efficiency. Consistently, the intensity of the residual fundamental light, I_F, can be written as $I_F = I - kI^2$. If we assume that the incoming light is described by a multimode thermal intensity distribution, that is the convolution of μ equally-populated thermal fields [13],

$$P_\mu(I) = \frac{e^{-I/(\langle I\rangle/\mu)}}{(\langle I\rangle/\mu)^\mu}\frac{I^{\mu-1}}{(\mu-1)!}, \tag{1}$$

having mean value $\langle I\rangle$, the statistics of the residual light becomes

$$\begin{aligned} P_F(I_F) &= P_\mu\left(\frac{1-a}{2k}\right)\frac{2k}{(1-2k)(1-a)} \\ &= \left(\frac{1-a}{2k}\right)^{\mu-1}\frac{e^{[-\mu(1-a)]/(\langle I\rangle 2k)}}{a(\langle I\rangle/\mu)^\mu(\mu-1)!}, \end{aligned} \tag{2}$$

in which $a = \sqrt{1-4kI_F}$, and we have assumed that all the modes μ are up-converted. If $k \ll 1$, it is possible to demonstrate that $P_F(I_F)$ is essentially indistinguishable from a

multimode thermal statistics apart from small corrections that tend to slightly increase the intensity fluctuations. By applying the well-known semiclassical theory of photodetection [13], the probability distribution of detected photons can be obtained, even if not analytically. By following the same procedure used for the residual light at the fundamental frequency, it is also possible to derive the expression of the SH intensity distribution:

$$P_{\mathrm{SH}}(I_{\mathrm{SH}}) = P_{\mu}(b)\frac{1}{2kb} = \frac{b^{(\mu-2)}e^{-\mu b/\langle I\rangle}}{2k(\mu-1)!(\langle I\rangle/\mu)^{\mu}}, \tag{3}$$

where $b = \sqrt{I_{\mathrm{SH}}/k}$. We note that the conversion efficiency k acts as a simple rescaling of the intensity I_{SH}, so that we can redefine $I_{\mathrm{SH}} \equiv I_{\mathrm{SH}}/k$. The corresponding probability distribution of detected photons reads as

$$\begin{aligned} P_{\mathrm{SH}}(m) &= \int_0^{\infty} \mathrm{d}I_{\mathrm{SH}} \frac{(\eta I_{\mathrm{SH}})^m}{m!} e^{-\eta I_{\mathrm{SH}}} P_{\mathrm{SH}}(I_{\mathrm{SH}}) \\ &= \frac{\Gamma[1/2+m+\mu/2]\Gamma[m+\mu/2]}{4\sqrt{\pi}m!(\mu-1)!\{\langle m\rangle/[\mu(1+\mu)]\}^{(\mu+1)/2}} \\ &\quad \times U\left[\frac{1}{2}+m+\frac{\mu}{2},\frac{3}{2},\frac{\mu(\mu+1)}{4\langle m\rangle}\right], \end{aligned} \tag{4}$$

in which η is the quantum detection efficiency, $\Gamma[j]$ is the Gamma function, $U[i,j,k]$ is the Tricomi confluent hypergeometric function, μ is the number of modes in the fundamental beam, and $\langle m\rangle$ is the mean number of detected photons. Note that in the second line of Eq. (4), we have put $\eta = 1$. This choice is motivated by the fact that the statistics under investigation is classical and thus invariant upon inefficient detection [11,14]. The result of Eq. (4) is interpreted as the actual distribution of detected photons. In this way, we lose the quantitative connection between the fundamental and up-converted intensities, but we retain the relation between their statistics. Mean value and variance of the distribution in Eq. (4) can be written as $\langle m\rangle = [(\mu+1)/\mu]k\eta\langle I\rangle^2$ and $\sigma^2(m) = \{2(2\mu+3)/[\mu(\mu+1)]\}\langle m\rangle^2 + \langle m\rangle$, respectively. If the SH light described by the above statistics is divided at a beam splitter (BS) of transmissivity τ, the expression of the correlation coefficient $C_{\mathrm{SH}} = (\langle m_1 m_2\rangle - \langle m_1\rangle\langle m_2\rangle)/\sqrt{[\sigma^2(m_1)\sigma^2(m_2)]}$ between the shot-by-shot detected photons m_1 and m_2 at the two outputs becomes [12]

$$\begin{aligned} C_{\mathrm{SH}} &= \frac{\sqrt{\tau(1-\tau)}[\sigma^2(m)-\langle m\rangle]}{\sqrt{[\tau\sigma^2(m)+(1-\tau)\langle m\rangle][(1-\tau)\sigma^2(m)+\tau\langle m\rangle]}} \\ &= \frac{\sqrt{\langle m_1\rangle\langle m_2\rangle}}{\sqrt{(\langle m_1\rangle+c)(\langle m_2\rangle+c)}}, \end{aligned} \tag{5}$$

where $c = [\mu(\mu+1)]/[2(2\mu+3)]$. Note that the same expression for the correlation coefficient holds in the case of multimode thermal light by substituting c with μ [12]. In the present case, since $c < \mu$ for all the values of μ, the state described by Eq. (5) is more correlated than a multimode thermal one with the same $\langle m\rangle$ and μ, though being still classical.

In order to experimentally test the difference between a multimode thermal statistics and a super-thermal one, in the following, we present data obtained in two different conditions. In the first case [see Fig. 1(a)], the ps-pulsed third-harmonics at

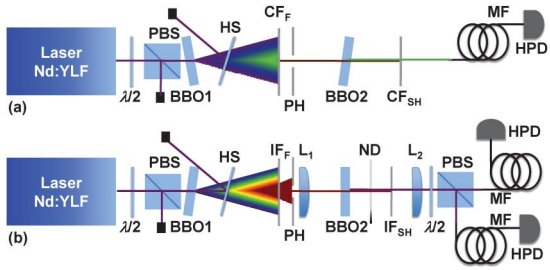

Fig. 1. Sketch of the experimental setups. (a) and (b) refer to the two experimental configurations. See the text for details.

349 nm (UV pump hereafter) of a mode-locked Nd:YLF laser regeneratively amplified at 500 Hz was used to produce PDC in a 4-mm-long BBO crystal (BBO1, 33.8-deg cut angle). A portion of the light around 1047 nm was selected by a pinhole (PH, 1-mm diameter), spectrally filtered (with a colored-glass filter, $\mathrm{CF_F}$) and sent to a 8-mm-long BBO crystal (BBO2, 28-deg cut angle), placed ~50 cm beyond the first crystal and properly tuned to produce second-harmonics. A colored-glass filter ($\mathrm{CF_{SH}}$) was used to completely remove the residual infrared light, whereas the SH light centered at 523 nm was delivered by a 300-μm-core multimode fiber (MF) to a hybrid photodetector (HPD, mod. R10467U-40, Hamamatsu, nominal quantum efficiency 50% at 523 nm). To perform a systematic characterization, the power of the UV pump was changed by means of a half-wave plate ($\lambda/2$) and a polarizing cube beam splitter (PBS) located in front of BBO1, and each experimental run was repeated 100,000 times for each choice of the pump power. In Fig. 2(a), we show a typical detected-photon distribution (gray columns) obtained by exploiting the self-consistent method already explained in Refs. [15,16]. The method yields the mean value of detected photons, $\langle m\rangle$, independent of any assumption about the distribution. We compare the experimental data with three possible probability distributions. First of all, we consider a Poissonian distribution having the same mean value as the data (blue dotted line + symbols) and obtain a bad superposition. Second, we fit the data with a multimode thermal distribution of fixed mean value, leaving the number of modes as the only fitting parameter. In this case, the best fit (red dashed line + symbols) returns an unphysical number of modes ($\mu<1$). Finally, we fit the data with the super-thermal distribution in Eq. (4) for fixed $\langle m\rangle$ and μ as the only fitting parameter. The resulting value for the number of modes in the fundamental up-converted to SH is $\mu \sim 3$. The better superposition of this last fit to data is testified by the larger value of fidelity parameter $f = \sum_{m=0}^{\overline{m}} \sqrt{P^{\mathrm{th}}(m)P(m)}$, in which $P^{\mathrm{th}}(m)$ and $P(m)$ are the theoretical and experimental distributions, respectively, and the sum extends up to the maximum number of detected photon $\overline{m}$ above which both $P^{\mathrm{th}}(m)$ and $P(m)$ become negligible (see the Inset of Fig. 2).

The chosen experimental configuration did not allow us to simultaneously monitor the residual infrared light due to the responsivity of HPDs, which are blind above 750 nm. A second experimental configuration was thus realized, in which both the investigated wavelengths, namely 700 and 350 nm, could be

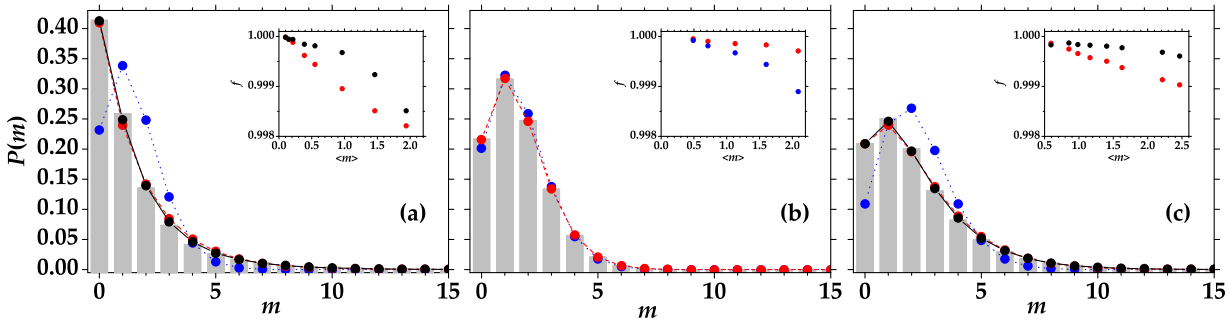

Fig. 2. Experimental detected-photon distribution (grey columns), Poissonian curve (blue dotted line + symbols), multimode thermal fit (red dashed line + symbols) and super-thermal fit (black solid line + symbols) for SH light around 523 nm (panel (a), mean value $\langle m\rangle = 1.46 \pm 0.01$), residual of fundamental light around 700 nm (panel (b), mean value $\langle m\rangle = 1.60 \pm 0.01$), and SH light around 350 nm (panel (c), mean value $\langle m\rangle = 2.21 \pm 0.01$). Error bars are smaller than the symbol size. Insets: fidelity values as functions of $\langle m\rangle$ for the fit to a Poissonian distribution (blue dots), to a multimode thermal distribution (red dots), and to a super-thermal distribution (black dots). Note that in panel (a) and (c), the fidelity values to a Poissonian distribution are not shown to better enhance the difference between the other two distributions.

detected by the HPD (nominal quantum efficiency ~30% at both wavelengths). As shown in Fig. 1(b), the same UV pump at 349 nm was used to generate PDC in an 8-mm-long BBO crystal (BBO1, 37-deg cut angle) in quasi-collinear interaction geometry. A portion of PDC light was spectrally filtered by a band-pass filter, IF_F, centered at 700 nm, and spatially selected by a pinhole (PH, 1-mm diameter) placed at ~80 cm beyond BBO1. The light passing through the pinhole was then collimated by a 500-mm focal-length lens (L_1) and injected in a second BBO crystal (BBO2, 4-mm long, 33.8-deg cut angle). Either the light around 700 nm or that around 350 nm was then focused by means of lens L_2 into a 600-μm-core multimode fiber (MF) used to deliver the light to the HPD. A variable neutral density filter (ND) placed behind BBO2 changed the mean value of light without changing the number of modes. For each choice of the filter attenuation, the experimental run was repeated 100,000 times. A typical example of detected-photon number distribution of the fundamental light around 700 nm is shown in Fig. 2(b). In the figure, the Poissonian curve, shown as blue dotted line + symbols, exhibits a bad superposition to the experimental data, whereas the multimode thermal fit (red dashed line + symbols) is well superimposed. Such a behavior testifies that, if the efficiency of the nonlinear process is low, the statistics of the residual light essentially remains multimode thermal. Note that 4.7 optical density filters were placed behind BBO2 to keep the values of the residual light within the dynamic range of the HPD detectors without changing the value of PDC gain during the measurement session. In panel (c) of Fig. 2, a typical detected-photon-number distribution of SH light around 350 nm is shown: the experimental data (gray columns) are presented together with the corresponding Poissonian curve (blue dotted line + symbols), the multimode thermal fit (red dashed line + symbols), and the super-thermal fit (black solid line + symbols). The last model better superimposes to the data, again testifying that the statistical properties of SH light are modified by the nonlinear interaction. Actually, in such a configuration the multimode thermal fit would not give unphysical values like in the previous case, since the number of modes in the fundamental distribution is larger. This difference with respect to the previous case can be ascribed to phase-matching conditions, which influence PDC properties. By fitting the SH with a multimode thermal distribution, we get roughly 2–3 modes, a result that is less reasonable than that obtained by the super-thermal model (8–9 modes), especially considering the number of modes (~20) measured in the residual light at the fundamental wavelength. Note that the intrinsic difference in the number of modes between fundamental and SH can be ascribed both to the nonflat spectral distribution of the PDC light and to the phase-matching conditions that operate a selection in the conversion efficiency of the different spectral components. Finally, by comparing the Insets of Figs. 2(a) and 2(c), we can notice that the smaller the number of modes, the bigger the difference between the multimode thermal statistics and the super-thermal one.

To highlight the difference in the statistical properties of SH light, we also decided to monitor the effect of photon-number fluctuations. To this aim, we divided the light at a polarizing cube beam splitter (PBS) preceded by a half-wave plate ($\lambda/2$). The two balanced outputs were then detected by two HPDs

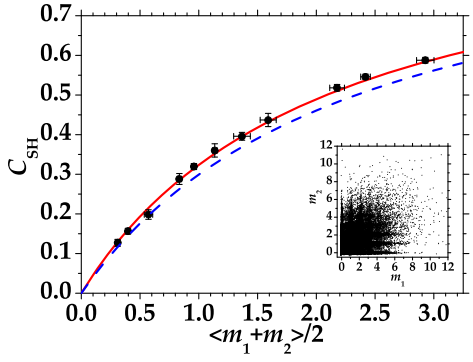

Fig. 3. Black dots: correlation coefficient C_{SH} as a function of the mean number of photons measured in the two arms of the PBS at which SH light around 350 nm is divided. Red solid line: theoretical expectation according to Eq. (5); blue dashed line: theoretical expectation for a multimode thermal state. Inset: number of detected photons in one arm as a function of the number of photons detected in the other arm.

(see the Inset of Fig. 3). In the main panel of Fig. 3, we show the behavior of the correlation coefficient [17] as a function of the mean number of photons in the two arms: it is clear that the experimental results, shown as dots, are in perfect agreement with the theoretical prediction based on the super-thermal model (red solid line), whereas they superimpose worse to the theoretical expectation based on a multimode thermal description (blue dashed line). We remark that in the expressions of the theoretical predictions, the mean value of the number of modes given by the fits of each detected-photon distribution was used to set the number of modes.

In conclusion, we demonstrated, both theoretically and experimentally, that if the multimode thermal PDC light undergoes SHG, the converted light exhibits larger fluctuations, whereas the statistics of the residual light at fundamental frequency can deviate from the original one only in the presence of non-negligible conversion efficiency. The perfect agreement between the experimental data and the theoretical predictions is shown both in terms of detected-photon-number distributions and correlation coefficient. Further investigations are now in progress with pseudo-thermal light to better keep under control the number of modes that are actually up-converted. This study is required to better understand the dynamics of SHG process and to possibly produce pump beams for PDC having statistical properties other than Poissonian. It could be interesting to investigate the effect of such a modified pump on the statistics of PDC. Moreover, this analysis will open new applicative perspectives. In fact, thanks to its multimode nature and its higher-than-thermal fluctuations, super-thermal statistics could be exploited to implement new ghost imaging protocols, whose performances can be directly compared with the results already obtained with multimode thermal light.

Funding. MIUR (RBFR10YQ3H).

Acknowledgment. The Authors thank Jan Peřina and Jan Peřina Jr. for fruitful discussions.

REFERENCES

1. P. A. Franken, A. E. Hill, C. W. Peters, and G. Weinreich, Phys. Rev. Lett. **7**, 118 (1961).
2. G. Barreto Lemos, V. Borish, G. D. Cole, S. Ramelow, R. Lapkiewicz, and A. Zeilinger, Nature **512**, 409 (2014).
3. J. E. Midwinter, Appl. Phys. Lett. **12**, 68 (1968).
4. J. S. Dam, P. Tidemand-Lichtenberg, and C. Pedersen, Nat. Photonics **6**, 788 (2012).
5. O. Jedrkiewicz, J.-L. Blanchet, E. Brambilla, P. Di Trapani, and A. Gatti, Phys. Rev. Lett. **108**, 253804 (2012).
6. B. Dayan, A. Peer, A. A. Friesem, and Y. Silberberg, Phys. Rev. Lett. **94**, 043602 (2005).
7. J. L. Debethune, Nuovo Cimento **12**, 101 (1972).
8. P. Chmela, Czech. J. Phys. B **38**, 283 (1988).
9. P. Chmela, Z. Ficek, and S. Kielich, Czech. J. Phys. B **39**, 509 (1989).
10. Y. Qu and S. Singh, Phys. Rev. A **51**, 2530 (1995).
11. M. Bondani, A. Allevi, and A. Andreoni, Adv. Sci. Lett. **2**, 463 (2009).
12. A. Allevi, M. Bondani, and A. Andreoni, Opt. Lett. **35**, 1707 (2010).
13. L. Mandel and E. Wolf, *Optical Coherence and Quantum Optics* (Cambridge University, 1995).
14. E. Casini and A. Martinelli, J. Math. Anal. Appl. **399**, 608 (2013).
15. M. Bondani, A. Allevi, A. Agliati, and A. Andreoni, J. Mod. Opt. **56**, 226 (2009).
16. A. Andreoni and M. Bondani, Phys. Rev. A **80**, 013819 (2009).
17. A. Agliati, M. Bondani, A. Andreoni, G. De Cillis, and M. G. A. Paris, J. Opt. B **7**, S652 (2005).